

Figure S1. Phylogenetic analysis of *csflr* paralogs in vertebrates. Phylogenetic relationships between zebrafish *csflra* and *csflrb* paralogs and vertebrate orthologs. Amino acid divergence based on maximum likelihood algorithm (500 replicates; ≥ 70 bootstrap shown as unique branch). In support of homology assessments, synteny between *csflra* and *csflrb* was analyzed across multiple vertebrate species. Data supports *csflrb* being an ohnologue of *csflra*, stemming from a teleost whole genome duplication of a common homologue.

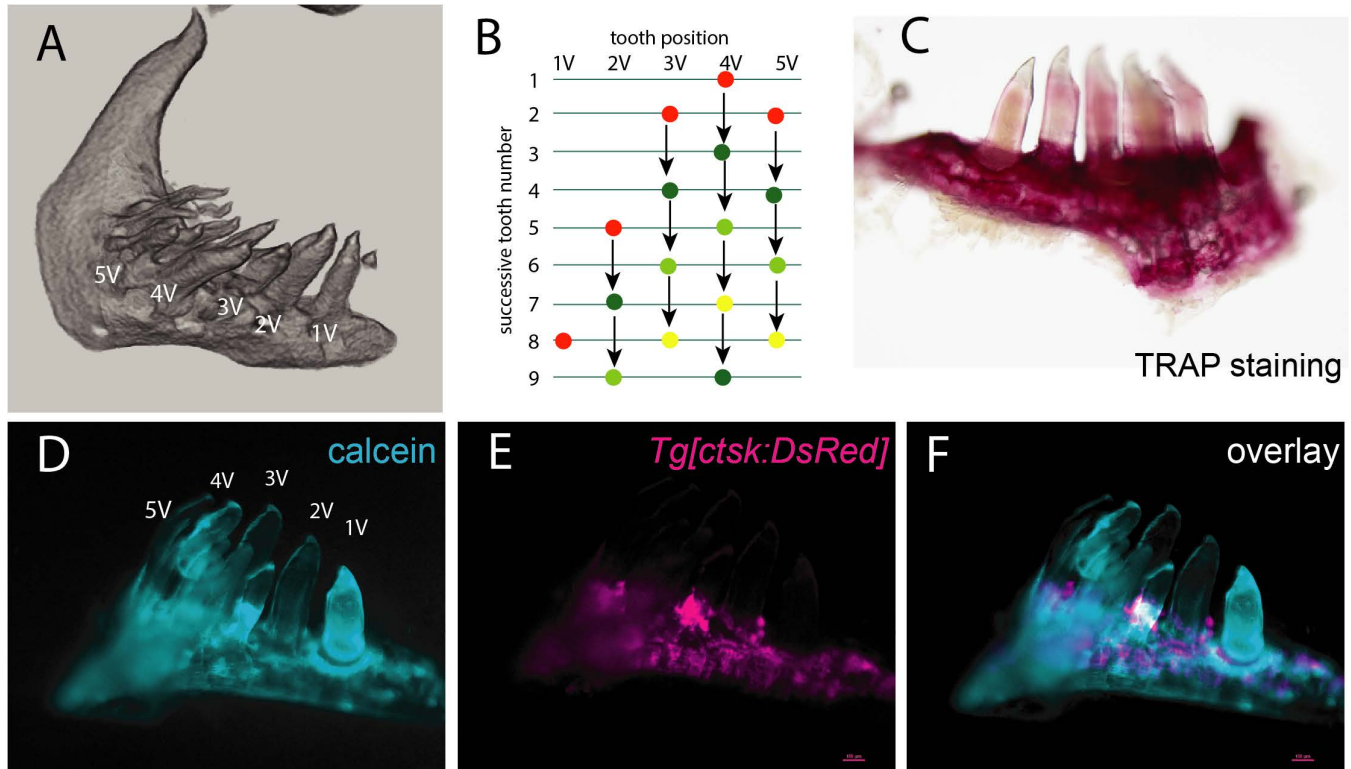


Figure S2. Generation of mutants in *csflr* paralogues in the zebrafish. (A) Clustering of zebrafish *csflr* genes with closely related receptor tyrosine kinases supports paralogous relationship between *csflra* and *csflrb*. (B-C) Schematic of the gene and protein structure of *csflr* genes indicating the position and consequence of the mutation. (B) The *csflra*^{mh5} allele of *csflra* is a G>T substitution at bp 1466 of the coding sequence predicted to result in a premature termination of the protein (E454X). (C) The *csflrb*^{mh108} mutant zebrafish allele is a combination of an 8bp insertion and a 4bp deletion within exon 3 due to targeted editing of the *csflrb* locus by CRISPR/Cas9. This change is predicted to cause a frameshift at amino acid 160 leading to a premature termination of the Csf1rb protein at amino acid 233 (P160L;fs73X). The *csflrb*^{mh112} mutant allele is a 13bp deletion within exon 3 resulting in a frameshift and premature termination of the Csf1rb protein at amino acid 161 (D159A;fs2X).

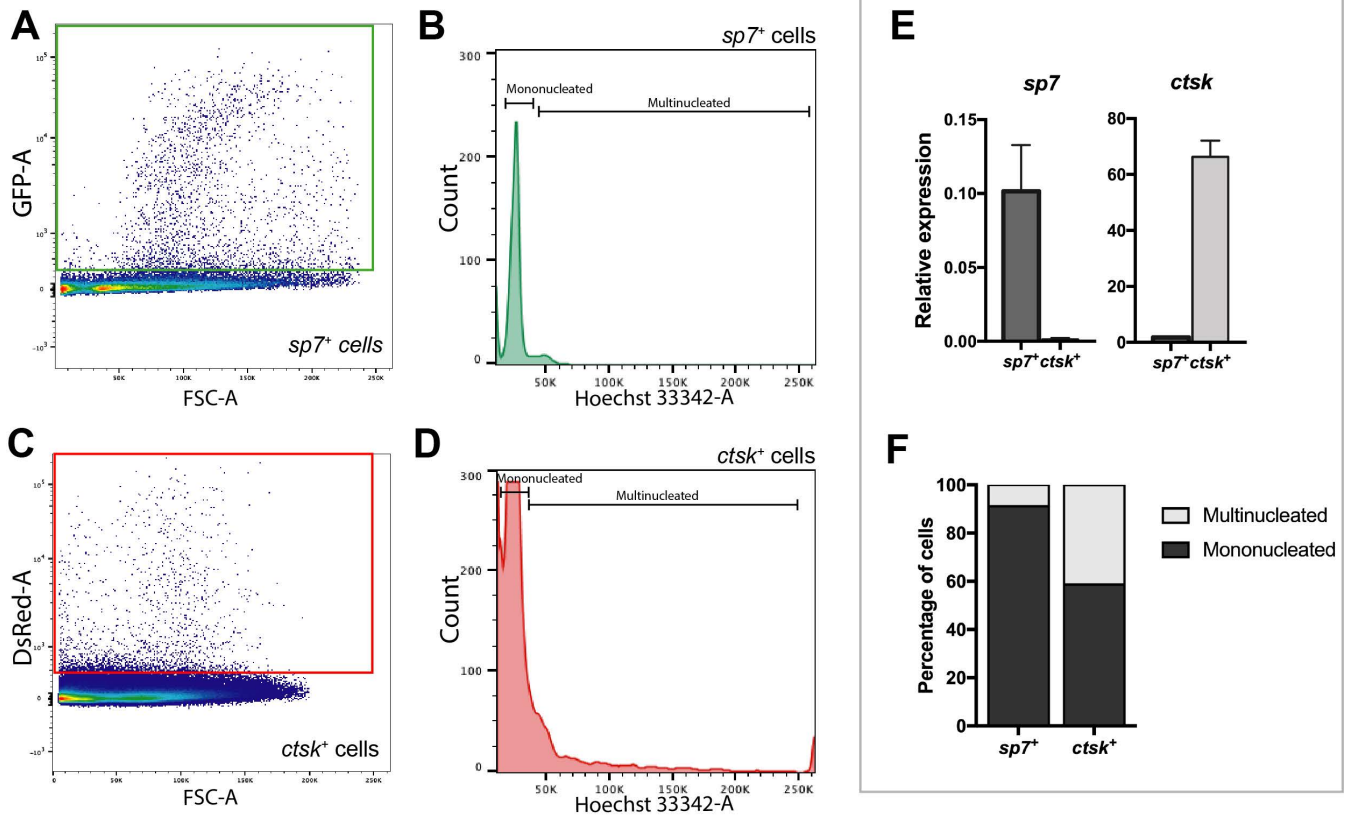


Figure S3. *CathepsinK* transgenic line specifically marks osteoclasts during late skeletal development in zebrafish. (A) Schematic detailing the construct used to generate an osteoclast reporter line expressing *DsRed* under the control of the medaka *cathepsin K* promoter. This construct has the capability to drive *Cre* recombinase expression by flippase-mediated recombination. (B-C) Expression of *Tg[ctsk;DsRed]* in opercula (B) and in the spine (C) of 2wpf zebrafish in comparison with sites of calcified bone as detected by calcein staining (cyan). (D) Co-localization of *DsRed* expression with TRAP staining in a 10wpf wild-type scale.

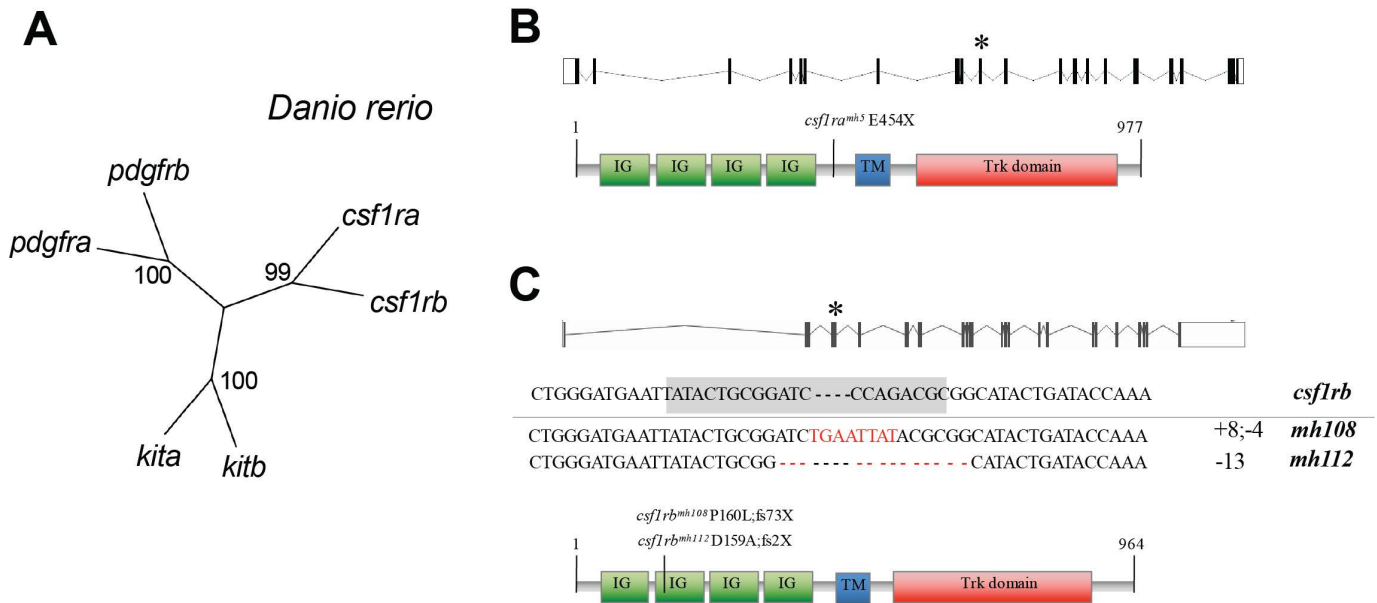


Figure S4. FACS isolation of osteoclasts and osteoblasts from adult zebrafish. (A, C) $sp7^+$ and $ctsk^+$ cells were isolated from adult $Tg[sp7:EGFP]$ and $Tg[ctsk:DsRed]$ fish, respectively, and identified by their expression of $EGFP$ (A) and $DsRed$ (C). (E) $EGFP^+$ and $DsRed^+$ cells were sorted and analyzed regarding their expression of $sp7$ and $ctsk$. (B, D) Cells were gated and analyzed for Hoechst 33342 expression. A Hoechst 33342 histogram was plotted and $sp7:EGFP^+$ cells were used to set the gating strategy for identification of mononucleated cells (B). Osteoblasts are traditionally mononucleated cells, so the small population that falls inside the multinucleated gate is due to higher DNA content during cell division. By applying the same gates to the $ctsk:DsRed^+$ cells we identified the multinucleated cell population (D). (F) The percentage of mononucleated and multinucleated cells was quantified for both fish lines.

	CREB/AP1	FOXO
Danio rerio	AAAGAGTGTGATTTCCGCGTCTGTCTGTGACTCAGATCTGGCTCTGCCCCCTTATTGAAACAGCTCTTCAGTCTCGCTGTAAACACATGATCCACTGCCAGGCCTGGATTTCCACACATTCACACTCATCCTCTCAGCTTTAGCCACGCC	
Danio aesculapii	AAAGAGTGTGATTTCCGCGTCTGTCTGTGACTCACA-----TCTGCCCTTTATTTATACAGATCTCCGTTCTGCTGTGAAACACATGATCCACTCCAAGGCCTGGATTTCCACACATTCACAC-----AGATTTAGCCACGCC	
Danio erythromicron	AAAAAGTGTGATTTCTGGCTCTGTCTGTGACTCAGATCTGGCTCTGCCCCCTTATTGAAACAGATCTTCGGTTCTGCTGTAAACACATGATCCACTGCCAGGCCTGGATTTCCACACATTCACACTTATCCTCTCAGCTTTATCCAGGCC	
Danio margaritatus	AAAAAGTGTGATTTCTGGCTCTGTCTGTGACTCAGATCTGGCTCTGCCCCCTTATTGAAACAGATCTTCAGTCTCGCTGTAAACACATGATCCACTGCCAGGCCTGGATTTCCACACATTCACACTTATCCTCTCTTTATCCAGGCC	
Danio nigrofasciatus	GAAAAGAGAGATTTCCGCGTCTGTCTGTGATTCAGATCTGGCTCTGCCCCCTTATTGAAACAGATCTTCAGTCTCGCTGTAAACACATGATCCACTGCCAGGCCTGGATTTCCACACATTCACACTCATCCTCTCAGCTTTAGCCAAAGCC	
Danio choprae	AAAAAGAGTGTGATTTCCGCGTCTGTCTGTGACTCAGATCTGGCTCTGCCCCCTTATTGAAACAGATCTTCAGTCTCGCTGTAAACACATGATCCACTGCCAGGCCTGGATTTCCACACATTCACACTCATCCTCTCAGCTTTAGCCACGCC	
Danio abollineatus	GAAGAGTGTGATTTCCGCGTCTGTCTGTGACTCAGATCTGGCTCTGCCCCCTTATTGAAACAGATCTTCAGTCTCGCTGTAAACACATGATCCACTGCCAGGCCTGGATTTCCACACATTCACACTCATCCTCTCAGCTTTAGCCACGCC	
Gadus morhua		TATCTTGATGGTGTGAGTCAGGCCTCCGTTCTGCCAGTTAGACACATGATCCCGAGCGAGGACCTT
Takifugu rubripes		TTGTTGTTTTGCTGTGAGTCAGGCCTCCGTTCTGCCAGTTAGCCACATGATCCGAGAGCTAAAAATCC
Tetraodon nigroviridis		TTCTTTGTTTTGCTGTGAGTCAGGCCTCCGTTCTGCCAGTTAGCCACATGATCCGAGAGCTAAAAATCC
Oreochromis niloticus		TTCTTTGTTTTGCTGTGAGTCAGGCCTCCGTTCTGCCAGTTAGCCACATGATCCGAGAGCTAGAGAGCC
Gasterosteus aculeatus		TTCTTTGTTTTGCTGTGAGTCAGGCCTCCGTTCTGCCAGTTAGCCACATGATCCGAGAGCTAGAGAGCC
Oryzias latipes		TTCTTTGTTTTGCTGTGAGTCAGGCCTCCGTTCTGCCAGTTAGCCACATGATCCGAGAGCTGGGATGCC
Poecilia formosa		TTCTTTGTTTTGCTGTGAGTCAGGCCTCCGTTCTGCCAGTTAGCCACATGATCCGAGAGCTGGGATGCC
Xiphophorus maculatus		TTCTTTGTTTTGCTGTGAGTCAGGCCTCCGTTCTGCCAGTTAGCCACATGATCCGAGAGCTGGGATGCC
Astyanax mexicanus		TTCTTTGTTTTGCTGTGAGTCAGGCCTCCGTTCTGCCAGTTAGCCACATGATCCGAGAGTCAGGCCTGCC

Figure S5. Pattern of osteoclast distribution on juvenile and adult vertebrae. (A-C)

Representative fluorescent photomicrographs of the spine of individual *csflr* mutants and wild-type siblings at 2wpf carrying the osteoclast reporter *Tg[ctsk:DsRed]* and counterstained with calcein (cyan). (D-F) At 4 months of age, spines of wt and individual *csflr* mutants exhibit a wide range of *ctsk:DsRed*⁺ cell numbers. Shown here are representative fluorescent photomicrographs of spines with high and low number of cells.

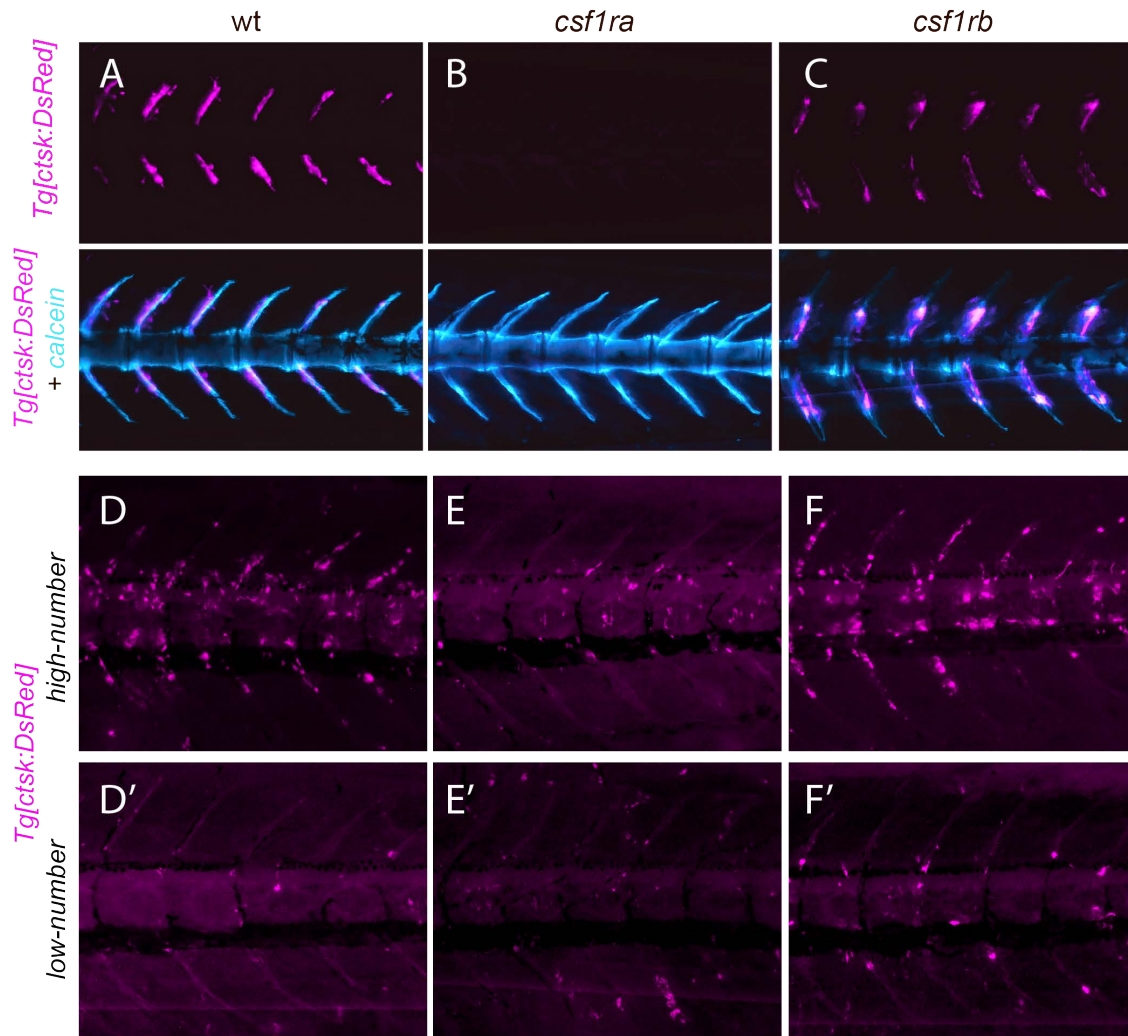


Figure S6. Tooth development and expression of osteoclast markers.

(A) MicroCT of the teeth bearing fifth ceratobranchial of the adult zebrafish. Tooth labeled 1V-5V in order of position. More medial teeth, 4M or 1D and 2D are not noted. (B) Diagram of timing of tooth formation and pattern of replacement (after (Huysseune and Witten, 2006)). Changes in color indicate sequential teeth replaced in a series. (C) Whole mount TRAP staining of ceratobranchial 5 of an adult zebrafish showing presence of active osteoclasts covering the extent of the arch. (D-F) Representative pictures of ceratobranchial 5 from *Tg[ctsk:DsRed]* transgenic adult fish, marking osteoclasts surrounding the dentition; (F) overlay of *ctsk*-marked cells (E) and mineralized tissue labeled with calcein (D).

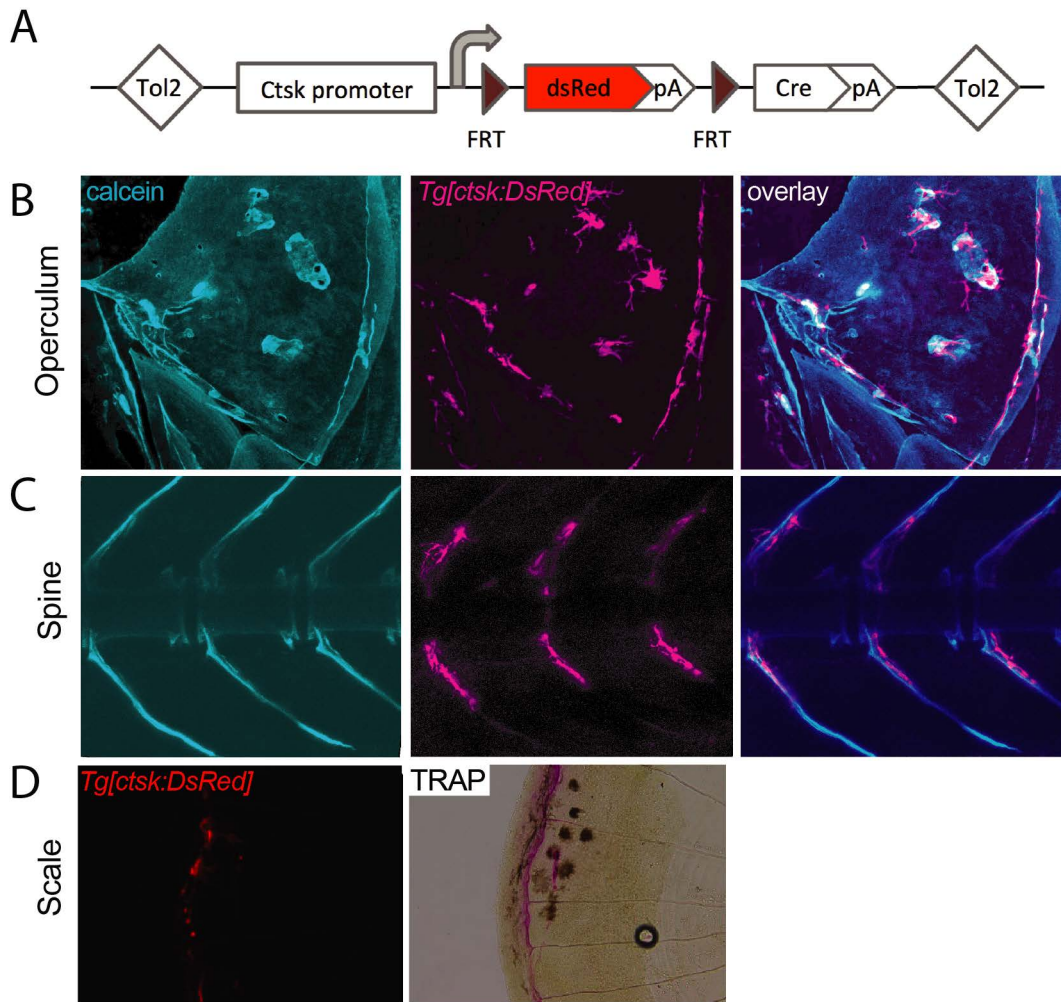


Figure S7. Multispecies alignment of *csf1ra* conserved non-coding element.

Yellow, conserved core regions common to all fishes; other colors are specific to the different teleost lineages. Sites of FOXO and CREB/AP1 binding site shown.

Table S1- Accession numbers of protein sequences used in the phylogenetic analysis.

Species	gene	Accession number
<i>Danio rerio</i>	<i>csflra</i>	NP_571747
	<i>csflrb</i>	F1QPE2
	<i>pdgfra</i>	F1QNY7
	<i>pdgfrβ</i>	A0A0G2L2B8
	<i>kita</i>	Q8JFR5
	<i>kitb</i>	B8A5K6
<i>Oryzias latipes</i>	<i>csflra</i>	H2LJC3
	<i>csflrb</i>	H2MBW3
<i>Takifugu rubripes</i>	<i>csflra</i>	H2SUK2
	<i>csflrb</i>	I6L6X5
<i>Astyanax mexicanus</i>	<i>csflra</i>	W5LCP3
	<i>csflrb</i>	W5KLJ6
<i>Oreochromis niloticus</i>	<i>csflra</i>	I3K5N3
	<i>csflrb</i>	I3KMS8
<i>Poecilia reticulata</i>	<i>csflra</i>	XP_008400061.1
	<i>csflrb</i>	XP_017158513.1
<i>Sinocyclocheilus grahami</i>	<i>csflra</i>	XP_016131860
	<i>csflrb</i>	XP_016102236
<i>Sinocyclocheilus rhinoceros</i>	<i>csflra</i>	XP_016426425
	<i>csflrb</i>	XP_016377545
<i>Sinocyclocheilus anshuiensis</i>	<i>csflra</i>	XP_016344784
	<i>csflrb</i>	XP_016361100
<i>Clupea harengus</i>	<i>csflra</i>	XP_012687948
	<i>csflrb</i>	XP_012669788
<i>Pygocentrus nattereri</i>	<i>csflra</i>	XP_017559280
	<i>csflrb</i>	XP_017575061
<i>Ctenopharyngodon idellus</i>	<i>csflra</i>	AKM12662
<i>Esox lucius</i>	<i>csflra</i>	XP_010895130
	<i>csflrb</i>	XP_01901945
<i>Salmo salar</i>	<i>csflra</i>	XP_014067972
	<i>csflra</i>	XP_014055375
	<i>csflrb</i>	XP_013985018
	<i>csflrb</i>	XP_014051429
<i>Cyprinodon variegatus</i>	<i>csflra</i>	XP_015246436
	<i>csflrb</i>	XP_015257023
<i>Latimeria chalumnae</i>	<i>csflr</i>	M3XGP0
<i>Xenopus tropicalis</i>	<i>csflr</i>	F6Z3F8
<i>Mus musculus</i>	<i>csflr</i>	P09581
<i>Homo sapiens</i>	<i>csflr</i>	NP_001275634

Table S2- Accession numbers of *csf1ra* genomic sequences used to retrieve CNE sequences.

Species		Accession number
<i>Danio</i>	<i>rerio</i>	ENSDARG00000102986
	<i>aesculapii</i>	D.Parichy (<i>unpublished</i>)
	<i>erythromicron</i>	
	<i>margaritatus</i>	
	<i>nigrofasciatus</i>	
	<i>choprae</i>	
	<i>abolineatus</i>	
<i>Takifugu rubripes</i>		ENSTRUG00000006553
<i>Tetraodon nigroviridis</i>		ENSTNIG00000014226
<i>Oreochromis niloticus</i>		ENSONIG00000013065
<i>Gasterosteus aculeatus</i>		ENSGACG00000018007
<i>Oryzias latipes</i>		ENSORLG00000004849
<i>Poecilia formosa</i>		ENSPFOG00000003496
<i>Xiphophorus maculatus</i>		ENSXMAG00000008588
<i>Astyanax mexicanus</i>		ENSAMXG00000017088